Transient heat conduction in a heat fin

Jed Brody and Max Brown
Department of Physics, Emory University, Atlanta, Georgia 30322

(Received 2 February 2016; accepted 4 May 2017)

We immerse the bottom of a rod in ice water and record the time-dependent temperatures at positions along the length of the rod. Though the experiment is simple, a surprisingly difficult problem in heat conduction must be solved to obtain a theoretical fit to the measured data. The required equipment is very inexpensive and could be assigned as a homework exercise or a hands-on component of an online course.
[http://dx.doi.org/10.1119/1.4983649]

I. INTRODUCTION

Heat fins are essential components of many familiar products, including electronic circuits[1] and engines.[2] Simply by providing additional surface area in contact with cool air, heat fins prevent overheating. Although the concept is simple, the mathematical details are complicated. Heat-fin experiments showcase practical applications of sophisticated mathematical techniques.

Here we present an inexpensive experiment that illustrates the complicated mathematical physics of transient heat conduction in fins. (We note here that "fin" suggests a shape with a thin rectangular cross section, but identical physics applies to rods with square or circular cross-sections.) In this work, we immerse the bottom of a rod in ice water (with the rest in air) and record the time-dependent temperatures at one or more positions along its length. This experiment requires only ice water, superglue, an Arduino Uno, a breadboard, and a temperature sensor,[3] all costing less than $30 (the rod can be a common nail). With the rise of online learning, science educators may be more and more obligated to identify meaningful experiments that online students can perform at home. Our experiment satisfies this criterion and is suitable for intermediate and advanced laboratory courses as well as courses in thermodynamics, heat transfer, engineering sciences, and even mathematical physics.

Previous papers describe other experiments involving heat conduction in rods. In some cases, convective heat transfer along the lengths of the rods was considered negligible,[4–9] but in our experiment, we will show that this assumption is not valid. In other papers, convective heat transfer along the length of the rod is accounted for,[10–12] but the boundary conditions for our experiment differ from those for previously described experiments. As such, the equation required to model our experiment has not, to our knowledge, been previously published.

II. THEORY

We will now derive the equation needed to fit our measured temperatures. We cannot use the one-dimensional heat equation,[1] $\partial^2 T/\partial x^2 = (1/\alpha)\partial T/\partial t$, because we need to account for convective heat transfer along the length of the rod. If there were no convective heat transfer between the rod and air, the entire rod would eventually reach thermal equilibrium with ice water, and this contradicts the measurements presented below.

Before solving a differential equation, we must first derive it; we do so by analyzing the differential volume element shown in Fig. 1. The thickness of the element is δx, and its cross-sectional area is A (perpendicular to the plane of the diagram and not shown).

The conductive heat transfer rate in through the top of the element is $q(x+\delta x)$, the conductive heat transfer rate out through the bottom of the element is $q(x)$, and the convective heat transfer rate out through the external surfaces of the element is q_{conv}. The net outward flow of heat causes the temperature to decrease according to

$$q(x+\delta x) - q(x) - q_{\mathrm{conv}} = (\rho A\, \delta x) c \frac{\partial T}{\partial t}, \tag{1}$$

where ρ is the mass density, T is temperature, and c is the specific heat. Equation (1) is simply the time derivative of the first law of thermodynamics applied to the differential volume element—because the work is zero, the net heat transfer rate equals the rate of change of internal energy.[1]

Expressing the heat transfer rates through Fourier's law of conduction and Newton's law of cooling, we obtain

$$kA\frac{\partial T(x+\delta x,t)}{\partial x} - kA\frac{\partial T(x,t)}{\partial x} - hP\,\delta x[T(x,t)-T_a] = (\rho A\,\delta x)c\frac{\partial T(x,t)}{\partial t}, \tag{2}$$

where T_a is the ambient temperature, k is the thermal conductivity, h is the heat transfer coefficient, and P is the perimeter of the cross-section. Dividing both sides by $kA\,\delta x$ and allowing $\delta x \to 0$ results in

$$\frac{\partial^2 T}{\partial x^2} - m^2(T-T_a) = \frac{1}{\alpha}\frac{\partial T}{\partial t}, \tag{3}$$

where $m = \sqrt{hP/kA}$ is called the fin parameter[1] and $\alpha = k/\rho c$ is the thermal diffusivity.

To solve Eq. (3), we need to know both the boundary conditions and the initial condition. The initial condition is that the rod is at ambient temperature, or

$$T(x,0) = T_a. \tag{4}$$

Immersing the bottom of the rod ($x=0$) in ice water causes convective heat flow into the ice water

$$k\frac{\partial T(0,t)}{\partial x} = h_0 T(0,t), \tag{5}$$

where h_0 is the heat transfer coefficient in ice water. Since water is a liquid, we expect h_0 to be an order of magnitude

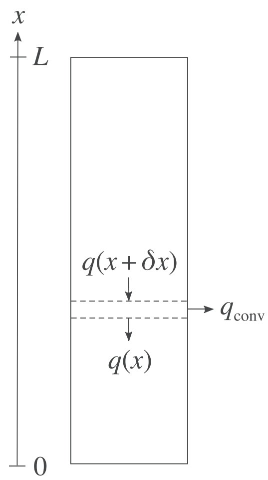

Fig. 1. Volume element of thickness δx within a rod of length L.

greater than h, the heat transfer coefficient in air.[13] The convective heat transfer at the top surface is therefore much less than the convective heat transfer at the bottom surface. In fact, we will neglect convective heat transfer at the top surface because the top surface area is small compared to the lateral surface area, and the temperature at the top surface is closest to ambient temperature. If the resulting theoretical expression fits our data, the approximation is justified. The approximation that convective heat transfer is zero at the top surface means that conductive heat transfer at the top surface must also be zero, requiring

$$\frac{\partial T(L,t)}{\partial x} = 0. \tag{6}$$

The steady-state temperature distribution is not uniform. Therefore, the solution to Eq. (3) must have a steady-state part $T_s(x)$ and a transient part $T_t(x,t)$, so that

$$T(x,t) = T_s(x) + T_t(x,t). \tag{7}$$

Equation (7) may be unfamiliar to students, but the concept is simple: the system evolves towards its steady-state solution, which does not depend on time. All of the time-dependence can therefore appear in a separate, transient term that decays to zero. Substituting Eq. (7) into Eq. (3) allows us to separate the steady-state fin equation,

$$\frac{d^2T_s}{dx^2} - m^2(T_s - T_a) = 0 \tag{8}$$

from the equation for the transient term,

$$\frac{\partial^2 T_t}{\partial x^2} - m^2 T_t = \frac{1}{\alpha}\frac{\partial T_t}{\partial t}. \tag{9}$$

The solution to Eq. (8) is $T_s(x) = T_a + ae^{mx} + be^{-mx}$, where a and b are coefficients to be determined by the boundary conditions, Eqs. (5) and (6). The final result is obtained through tedious yet straightforward algebra, giving

$$T_s(x) = T_a - \frac{h_0 T_a \cosh[m(L-x)]}{h_0\cosh(mL) + mk\sinh(mL)}. \tag{10}$$

Note that as h_0 gets very large, $T_s(0)$ approaches 0; highly effective convective heat transfer at the bottom surface of the rod reduces the temperature there to that of ice water. Conversely, as h_0 gets very small, the temperature of the rod remains at ambient temperature, unaffected by the ice water.

The transient equation is solved by separation of variables,[13] setting $T_t(x,t) = X(x)\tau(t)$, where $X(x)$ and $\tau(t)$ are functions to be determined. Substituting this expression into Eq. (9) and dividing by $X\tau$ yields $X''(x)/X = m^2 + \tau'(t)/\alpha\tau$, where the primes denote differentiation with respect to the function's argument. The left-hand side of this equation is a function of x while the right-hand side is a function of t, and the only way for a function of x to equal a function of t is if both functions are equal to the same constant, which we will call $-\lambda^2$. Then, solving the ordinary differential equation for $\tau(t)$ yields $\tau(t) = C\exp[-\alpha(m^2+\lambda^2)t]$, where C is an unknown coefficient. Meanwhile, the equation for $X(x)$ is solved by sinusoidal functions, which must satisfy the boundary conditions given in Eqs. (5) and (6). Equation (6) is satisfied if $X(x)$ has the form $\cos[\lambda(L-x)]$, and Eq. (5) then requires $\cot(\lambda L) = k\lambda/h_0$. A solution for $T_t(x,t)$ thus takes the form $C\exp[-\alpha(m^2+\lambda^2)t]\cos[\lambda(L - x)]$, and a sum over all possible λ is required to satisfy the initial condition, $T(x,0) = T_s(x) + T_t(x,0) = T_a$, so that $T_t(x,0) = T_a - T_s(x) = h_0 T_a\cosh[m(L-x)]/[h_0\cosh(mL) + mk\sinh(mL)]$. Expressing this function as a Fourier series[1] allows us to determine the coefficients C and obtain

$$\begin{aligned} T_t(x,t) = {} & \frac{2T_a h_0 \sinh(mL)}{h_0\cosh(mL) + mk\sinh(mL)} \\ & \times \sum_{n=1}^{\infty} \frac{\lambda_n[m\cos(\lambda_n L) + \lambda_n \sin(\lambda_n L)]}{[\lambda_n L + \cos(\lambda_n L)\sin(\lambda_n L)]\left(m^2+\lambda_n^2\right)} \\ & \times \cos[\lambda_n(L-x)]e^{-\alpha\left(m^2+\lambda_n^2\right)t}, \end{aligned} \tag{11}$$

where λ_n are the positive solutions to

$$\cot(\lambda_n L) = \frac{k\lambda_n}{h_0}. \tag{12}$$

As Eq. (12) is a transcendental equation, it must be solved numerically. The complete solution is finally obtained by substituting Eqs. (10) and (11) into Eq. (7).

This heat conduction problem is more advanced than typical heat conduction problems introduced in an undergraduate math methods course. Students may be amazed that such a simple experiment requires such complicated mathematics, and such an experiment may motivate and reward students' development of advanced mathematical skills.

Radiative heat transfer is not explicitly included here because it is much less important than convective heat transfer.[12] Even if radiative heat transfer is significant, the heat transfer coefficient can approximate the effects of both convective and radiative heat transfer.[13] To demonstrate this fact, we perform a Taylor series expansion on the exact expression for radiative heat transfer,

$$q_{rad} = e\sigma P\,\delta x(T^4 - T_a^4), \tag{13}$$

where e is the emissivity of the material, σ is the Stefan-Boltzmann constant, and $P\ \delta x$ is again the external surface area of a volume element of the material. The second-order Taylor series expansion around $T = T_a$ is

$$q_{\rm rad} = 4T_a^3 e\sigma P\,\delta x(T - T_a) + 6T_a^2 e\sigma P\,\delta x(T-T_a)^2. \tag{14}$$

If only the first-order term is retained, the coefficients can be absorbed into the convective heat transfer coefficient, which also multiplies $(T - T_a)$. The absolute value of the ratio of the second-order term to the first order term is $1.5(T_a - T)/T_a$, where $T_a = 293\,\text{K}$ and $T_a - T < 10\,\text{K}$ for all our experiments. The second-order term is therefore less than $1.5(10\,\text{K})/(293\,\text{K}) = 5.1\%$ of the first-order term, which is why little error is introduced by dropping the second (and higher) order terms.

III. EXPERIMENT

We used a 3.5 cm-long nail (including the head but not the tapering tip) with a diameter of 2.3 mm, and two 6 in.-long square rods of widths 0.25 in. and 0.75 in. composed of type 304 stainless steel. We superglued a single temperature sensor (Analog Devices TMP36)[14] into the head of the nail and three sensors along the length of each rod. The area of the sensor in contact with the material is a square with side length 4.5 mm. These sensors generate a voltage that depends linearly on temperature according to[14]

$$V = (10\,\text{mV}/^{\circ}\text{C})T + 500\,\text{mV}. \tag{15}$$

The sensors' leads were plugged into a breadboard, which was held in a clamp over a bowl of ice water, and were wired directly to an Arduino Uno. Each sensor has three leads: one connected to ground, one connected to 5 V, and one connected to an analog input, as shown in Fig. 2. We found that the sensors were sensitive to electrical noise, so to prevent anomalous results we avoided excessively long wires. The apparatus is shown in Fig. 3.

We immersed the bottom surfaces of the rods and the bottom portion of the nail in ice water. The nail was immersed to the level where it began to taper, designated as $x = 0$; above that level, the nail was considered to be a rod of approximately uniform cross-sectional area up to the top of the head at $x = L$. Every 5 s, we averaged 100 measurements from each sensor to obtain the temperature. In all, 100 measurements were completed within about 0.01 s, so the averaging does not result in any significant loss of time resolution. In all cases, data are read into a computer through an Arduino microcontroller. Lengthy instruction in Arduino programming is not required, as the necessary code is simple. The program requires little more than an analog read, a "serial print" of the data to the computer, and a delay to set the time interval between measurements.[15] Students are often amazed at how quickly and easily they learn how to interface with a sensor.

Our ultimate goal is to experimentally test our mathematical model, and to determine the thermal diffusivity α, the fin parameter m, and the heat transfer coefficient in ice water, h_0. For type 304 stainless steel, $\rho = 8{,}030\,\text{kg/m}^3$ and $c = 0.5\,\text{kJ/kg K}$ over a wide temperature range,[16] and k varies[17] from 14.4 W/K m at 0 °C to 14.8 W/K m at 20 °C. Therefore, α for the rods[18] should be about $4\,\text{mm}^2/\text{s}$. We are not certain of the composition of the nail, and thermal conductivity for different steel alloys varies[19] from 11–65 W/K m at 0 °C, so we expect α for the nail to be in the range of 2.7–$16\,\text{mm}^2/\text{s}$.

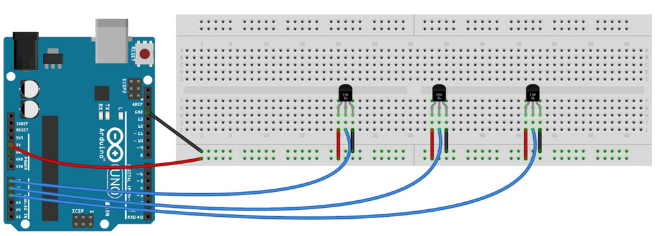

Fig. 2. Schematic diagram showing how the temperature sensors are connected to the Arduino (created using the open-source *Fritzing* program).

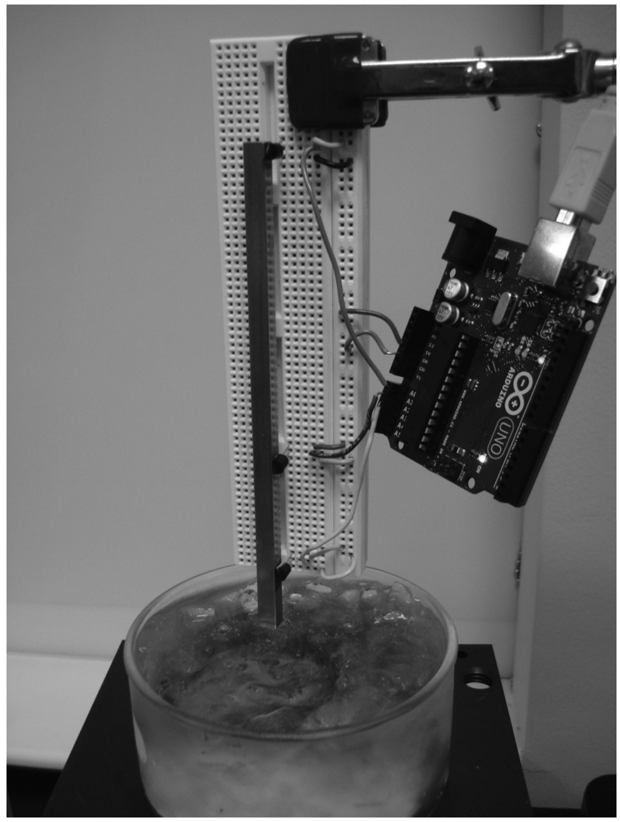

Fig. 3. The simple apparatus used to record temperatures at three locations along a 0.25 in.-wide steel rod.

The fin parameter m depends on physical dimensions, thermal conductivity, and the (unknown) heat transfer coefficient. The heat transfer coefficient in air can vary widely, though typical values[13] are in the range 5–$30\,\text{W/m}^2\,\text{K}$. Therefore, we expect m to be in the range 12–$69\,\text{m}^{-1}$ for the nail, 15–36 for the 0.25 in.-wide rod, and 8–21 for the 0.75 in.-wide rod. Meanwhile, our expectation is that h_0 will fall within a typical range[13] of the heat transfer coefficient for water, 30–$300\,\text{W/m}^2\,\text{K}$.

According to the data sheet for the temperature sensors,[14] the typical accuracy is ±1 °C, although it may be as poor as ±3 °C. We found that each sensor recorded very consistent values of room temperature, usually with a standard deviation less than 0.1 °C. However, the sensors differed by up to 3 °C from one another and from a digital thermometer measuring room temperature (20 °C). We assumed that the sensors could be calibrated by a simple additive correction, so if the initial temperature of a sensor was T_i, we added $(20\,^{\circ}\text{C} - T_i)$ to every measurement to obtain calibrated temperatures.

To fit the data using our mathematical model, we used the curve-fitting tool in MATLAB, though identical calculations can be performed using PYTHON or some other analysis program. We found that the series in Eq. (11) converged rapidly, and we truncated the series after 10 terms.

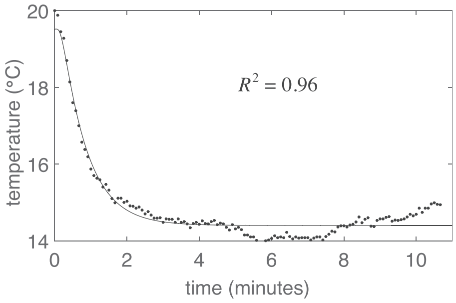

Fig. 4. Measured data and theoretical fit for the temperature at the top of a 3.5-cm nail.

IV. RESULTS AND DISCUSSION

Experimental results for the nail are shown in Fig. 4, along with a fit from the model. Although we are not certain of the composition of the nail, we assume that is stainless steel, and for density and specific heat, we use the values of type 304 stainless steel ($\rho = 8{,}030\,\mathrm{kg/m^3}$ and $c = 0.5\,\mathrm{kJ/kg\,K}$). The fitting parameters obtained were $\alpha = (1.4 \pm 0.4)\ \mathrm{mm^2/s}$, $m = (33 \pm 5)\ \mathrm{m^{-1}}$, and $h_0 = 1{,}500 \pm 400\,\mathrm{W/m^2\,K}$. Here, h_0 is five times larger than the largest typical value for water reported in the literature. We believe h_0 is anomalously high partly because the nail is not a perfect cylinder but also because the entire tapered tip was immersed, which dramatically increases the surface area in contact with the ice water as compared with a circular cross section. Because our model does not account for the geometry of the tip, the increased area for convective heat transfer manifests as an anomalously large convective heat transfer coefficient. The geometric deviation from the mathematical model is probably also responsible for the unexpectedly low value of α; it is about half the smallest typical value reported for steel.

The final temperature at the top of the nail is greater than $14\,^\circ\mathrm{C}$, demonstrating that convective heat transfer along the length of the nail is significant: if heat transfer occurred only between the ice water and the nail, the nail would eventually come into equilibrium with the ice water at $0\,^\circ\mathrm{C}$.

Experimental results, along with a fit using the model, for the thin square rod are shown in Fig. 5, with the fit parameters given in Table I. The values for α are all within 33% of the expected value of $4\,\mathrm{mm^2/s}$. In light of the approximations used in the mathematical model—α and k actually depend on temperature and are only approximately constant and uniform; similarly, h and m are also only approximately constant and uniform—we feel that such results are reasonably good. In fact, because the local heat transfer coefficient can vary so widely from one position to another, the symbol $\bar{h}$ is often used to represent the average heat transfer coefficient over a surface.[1] (We believe that such variability also accounts for the differences obtained for m and h_0.) The values of m provided in Table I fall within the expected range whereas the values of h_0 are much more variable. Note that at the position farthest from the ice water, the temperature changed by less than $1\,^\circ\mathrm{C}$, and the fit was unable to precisely specify h_0.

Table I. Fitting parameters obtained from temperatures taken at three positions on a 0.25 in.-wide steel rod.

Position x (cm)	α ($\mathrm{mm^2/s}$)	m ($\mathrm{m^{-1}}$)	h_0 ($\mathrm{W/m^2\,K}$)
14.95	3.9 ± 0.6	24 ± 2	800 ± 900
5.75	4.9 ± 0.4	18.5 ± 0.9	270 ± 20
2.1	2.7 ± 0.3	31 ± 2	450 ± 30

Results for the thick square rod are shown in Fig. 6 and Table II. The temperature data at the position farthest from the water clearly illustrate that the temperature does not follow a simple exponential decay; significant time elapses before the top of the rod is affected by the ice water. The goodness of the fits in Fig. 6 are very high, especially for the two lower positions. In addition, the fit parameters in Table II are much more consistent than for the thin square rod. As with the previous results, values obtained for α fall within 40% of the expected result. The values obtained for m are surprisingly close to one another, and are within the expected range. In addition, two of the values obtained for h_0 fall within the expected range, while the third is just 10% higher than expected.

V. CONCLUSIONS

We have demonstrated an inexpensive, experimentally simple but mathematically advanced laboratory-exercise that can be performed at home by online students. The mathematical model fits the measured data with a coefficient of determination that usually exceeds 0.98. By fitting the model to the measured data, we obtained thermal diffusivity values within 40% of the expected result. We consider this a

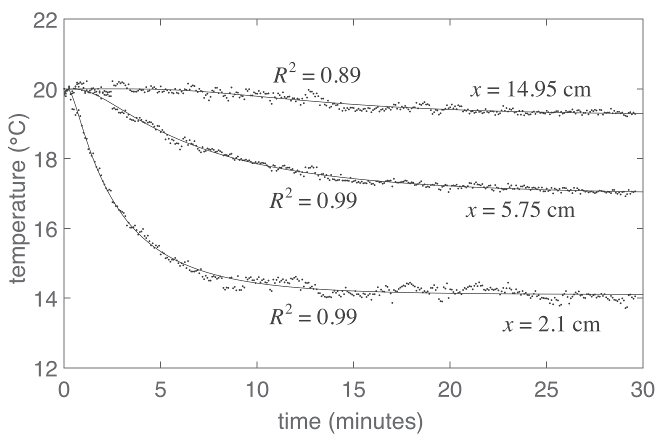

Fig. 5. Measured data and theoretical fits for the temperatures measured at three positions along a 0.25 in.-wide steel rod.

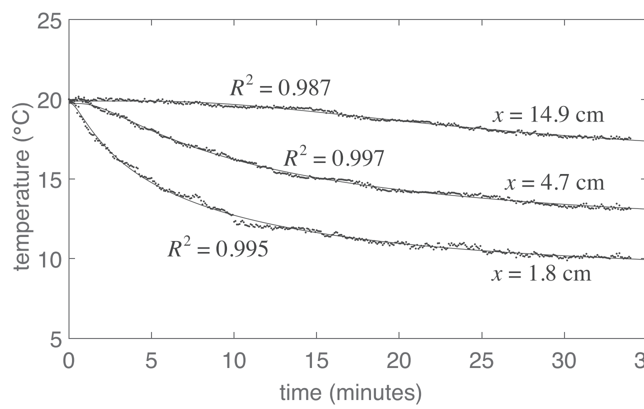

Fig. 6. Measured data and theoretical fits for the temperatures measured at three positions along a 0.75 in.-wide steel rod.

Table II. Fitting parameters obtained from temperatures taken at three positions on a 0.75 in.-wide steel rod.

Position x (cm)	α (mm^2/s)	m (m^{-1})	h_0 (W/m^2 K)
14.9	3.50 ± 0.16	12.5 ± 0.5	390 ± 70
4.7	2.89 ± 0.08	12.2 ± 0.3	306 ± 10
1.8	2.41 ± 0.10	12.5 ± 0.5	257 ± 5

success because the model equation relies on a significant assumption that the physical parameters—thermal conductivity, thermal diffusivity, heat transfer coefficient, and fin parameter—are all uniform and constant along the length of the rod.

ACKNOWLEDGMENT

Thanks to the rigorous demands and generous patience of the reviewers, this paper underwent a complete and necessary transformation.

[1]J. Lienhard and J. Lienhard, *A Heat Conduction Textbook*, 2nd ed. (Phlogiston Press, Cambridge, MA, 2012).

[2]A. E. Biernmann and H. H. Ellerbrock, Jr., "The design of fins for air-cooled engines," National Advisory Committee for Aeronautics (1941), pp. 401–424.

[3]The Arduino Uno and the Analog Devices temperature sensor TMP36GT9Z are available at <www.digikey.com>.

[4]C. H. Shaw and N. Saunders, "Intermediate laboratory experiment in heat conduction," Am. J. Phys. **23**, 89–90 (1955).

[5]H. G. Jensen, "Kohlrausch heat conductivity apparatus for intermediate or advanced laboratory," Am. J. Phys. **38**, 870–874 (1970).

[6]J. N. Fox and R. H. McMaster, "Measurement of the thermal properties of a metal using a relaxation method," Am. J. Phys. **43**, 1083–1086 (1975).

[7]J. H. Talpe, V. I. Bekeris, and C. E. Acha, "Measurement of thermal conductivity and heat capacity in an undergraduate physics laboratory," Am. J. Phys. **58**, 379–381 (1990).

[8]J. Brody, P. Andreae, and C. A. Robinson, "A simple optical probe of transient heat conduction," Am. J. Phys. **78**, 529–531 (2010).

[9]M. S. Anwar *et al.*, "Fourier analysis of thermal diffusive waves," Am. J. Phys. **82**, 928–933 (2014).

[10]A. B. Donaldson and A. R. Shouman, "Unsteady-state temperature distribution in a convecting fin of constant area," Appl. Sci. Res. **26**, 75–85 (1972).

[11]I. Rafols and J. Ortin, "Heat conduction in a metallic rod with Newtonian losses," Am. J. Phys. **60**, 846–852 (1992).

[12]M. C. Sullivan, B. G. Thompson, and A. P. Williamson, "An experiment on the dynamics of thermal diffusion," Am. J. Phys. **76**, 637–642 (2008).

[13]Y. Yener and S. Kakac, *Heat Conduction*, 4th ed. (Taylor and Francis Group, New York, 2008).

[14]The reference sheet for Analog Devices temperature sensor TMP36 is available at: <http://www.analog.com/media/en/technical-documentation/data-sheets/TMP35_36_37.pdf>.

[15]See supplementary material at http://dx.doi.org/10.1119/1.4983649 for Our Arduino code.

[16]AK Steel 304/304L Stainless Steel Data Sheet; <http://www.aksteel.com/pdf/markets_products/stainless/austenitic/304_304l_data_sheet.pdf>.

[17]C. Y. Ho and T. K. Chu, "Electrical resistivity and thermal conductivity of nine selected AISI stainless steels," Center for Information and Numerical Data Analysis and Synthesis Report 45, Purdue University, Sept. 1977.

[18]*Selected Cryogenic Data Notebook*, edited by J. E. Jensen *et al.* (Brookhaven National Laboratory, Upton, New York, Revised August 1980).

[19]*CRC Handbook of Chemistry and Physics*, edited by D. R. Lide, 75th ed. (CRC Press, Boca Raton, 1994).

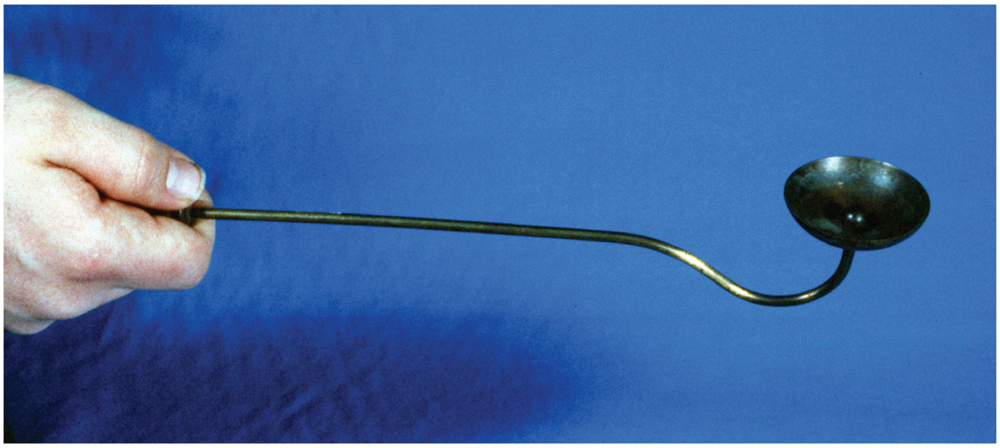

Spoon for Igniting Ether

Unlike Volta's Pistol or the Powder Bomb, the aim of this demonstration is not the loud explosion, but showing the ability of the electrical spark to start a fire in a flammable substance. The ether is held in the cup on the end of the handle, and a spark from a Leiden jar is allowed to jump to the edge of the cup that has been moistened with ether. The demonstration can also be done with alcohol. This apparatus is at Grinnell College in Iowa. There is no maker's name; similar apparatus was $1.00 in the 1888 Queen catalogue and $0.55 in the 1912 catalogue of C. H. Stoelting of Chicago. (Picture and Notes by Thomas B. Greenslade, Jr., Kenyon College)